Chapter 12

Automated Cell-by-Cell Tissue Imaging and Single-Cell Analysis for Targeted Morphologies by Laser Ablation Electrospray Ionization Mass Spectrometry

Hang Li, Brian K. Smith, Bindesh Shrestha, László Márk, and Akos Vertes

Abstract

Mass spectrometry imaging (MSI) is an emerging technology for the mapping of molecular distributions in tissues. In most of the existing studies, imaging is performed by sampling on a predefined rectangular grid that does not reflect the natural cellular pattern of the tissue. Delivering laser pulses by a sharpened optical fiber in laser ablation electrospray ionization (LAESI) mass spectrometry (MS) has enabled the direct analysis of single cells and subcellular compartments. Cell-by-cell imaging had been demonstrated using LAESI-MS, where individual cells were manually selected to serve as natural pixels for tissue imaging. Here we describe a protocol for a novel cell-by-cell LAESI imaging approach that automates cell recognition and addressing for systematic ablation of individual cells. Cell types with particular morphologies can also be selected for analysis. First, the cells are recognized as objects in a microscope image. The coordinates of their centroids are used by a stage-control program to sequentially position the cells under the optical fiber tip for laser ablation. This approach increases the image acquisition efficiency and stability, and enables the investigation of extended or selected tissue areas. In the LAESI process, the ablation events result in mass spectra that represent the metabolite levels in the ablated cells. Peak intensities of selected ions are used to represent the metabolite distributions in the tissue with single-cell resolution.

Key words Mass spectrometry, Imaging, Single-cell analysis, Cell-by-cell imaging, Metabolites, Tissue imaging, Molecular imaging

1 Introduction

Mass spectrometry imaging (MSI) is a rapidly emerging technique that enables the visualization of two- and three-dimensional distributions of metabolites, lipids, and proteins in biological tissues [1–5]. It complements the capabilities of conventional molecular histology by directly correlating molecular distributions with the histological features obtained from microscopy [1]. Established methods, such as MSI by matrix-assisted laser desorption ionization (MALDI) [6], and novel methods based on atmospheric pressure ionization, such as desorption electrospray ionization (DESI) [7]

Lin He (ed.), *Mass Spectrometry Imaging of Small Molecules*, Methods in Molecular Biology, vol. 1203,
DOI 10.1007/978-1-4939-1357-2_12,

and laser ablation electrospray ionization (LAESI) [8, 9], have demonstrated their ability to image diverse biological tissues. In most existing studies, MSI is performed by sampling based on a predefined gridding algorithm that follows a geometric pattern and ignores the cellular structure of the tissue [6, 7, 9–11]. As a consequence, molecular information from multiple cells may be captured together and cellular differences can be obscured [12].

As cells are the structural and functional units within a tissue, they represent the natural selection for pixels and voxels for two- and three-dimensional molecular imaging, respectively. To utilize this concept in MSI, analysis methods are needed for single-tissue-embedded cells. Optical fiber-based laser ablation in LAESI-MS can sample individual cells in their native environment [13, 14]. Using this method, cell-by-cell molecular imaging of metabolites in plant epidermal tissue was demonstrated [15]. Imaging was performed by manually moving the sample stage between cells. Manual control of the stage movement, however, is not feasible for the analysis of numerous single cells or selected cell types in extended tissue areas. Image processing combined with automating cell-by-cell imaging can overcome these limitations and provide a stable and efficient way to locate cells for analysis, thus enabling the investigation of extended or selected tissue areas. In this chapter, we present a protocol for automated cell-by-cell imaging of biological tissues using optical fiber-based laser ablation in LAESI-MS.

The procedure consists of the following major steps. Initially the tissue is inspected by an optical microscope and an image of the relevant area is captured. This image is processed to identify the coordinates of the cell centroids. These coordinates are used to program an automated translation stage that presents the individual cells one by one to the etched end of the optical fiber for ablation by the laser pulses. The plumes from the cell ablations are ionized by an electrospray and the produced ions are detected by a mass spectrometer. The peak intensities in the recorded mass spectra are used to create metabolite-specific ion intensity maps using the cells as pixels.

2 Materials

2.1 Reagents and Chemicals

1. Electrospray solution for ionization in positive ion mode: methanol with 0.1 % acetic acid (*v/v*):HPLC-grade water (1:1, *v/v*).
2. 1-Methyl-2-pyrrolidinone.
3. Germanium oxide (GeO_2)-based glass optical fiber (450 μm core diameter, Infrared Fiber Systems Inc., Silver Spring, MD, USA) (*see* Subheading 3.1).
4. Sapphire scribe.

5. Bare fiber chuck (BF300, Siskiyou Corporation, Grants Pass, OR, USA).
6. A translation stage (Thorlabs, Newton, NJ, USA).
7. Nitric acid: 1.0–2.4 % (*v/v*) reagent grade.

2.2 Biological Samples

1. Plant tissues such as Easter lily (*Lilium longiflorum*), leek (*Allium ampeloprasum*) and onion (*Allium cepa*) bulb.
2. Microtome knife blades for tissue excising.
3. Pre-cleaned microscope glass slides.

2.3 Cell Coordinate Recognition

1. An upright optical microscope (BX51, Olympus America Inc., Center Valley, PA, USA) was used for the imaging of cells in plant tissues.
2. Software used for image processing and cell coordinate measurements included ImageJ (Version 1.40 g, National Institute of Health, Bethesda, MD, USA) and MetaMorph for Olympus (Version 7.5.6.0, Olympus America Inc., Center Valley, PA, USA).

2.4 Single-Cell LAESI-MS

2.4.1 Microscope Visualization System

1. A homebuilt long-distance microscope, comprising a 7× precision zoom optic (Edmund Optics, Barrington, NJ, USA), a 2× infinity corrected objective lens (M Plan Apo 2×, Mitutoyo, Kanagawa, Japan), and a digital camera (Marlin F131, Allied Vision Technologies, Stadtroda, Germany), was mounted to provide a top view of the sample and the fiber tip and visualize the targeting and laser ablation of individual cells.
2. A similar long-distance microscope, built with the 7× precision zoom optic (Edmund Optics, Barrington, NJ, USA), a 5× infinity corrected objective lens (M Plan Apo 5×, Mitutoyo, Kanagawa, Japan), and a digital camera (Marlin F131, Allied Vision Technologies, Stadtroda, Germany), was positioned at a shallow angle to the sample (side view) to monitor the distance between the fiber tip and the sample surface. Positioning the fiber tip approximately a tip diameter away from the surface enabled effective laser ablation without fiber breakage.

2.4.2 Electrospray

1. The electrospray assembly components included an emitter (i.d. 50 μm, MT320-50-5-5, New Objective, Woburn, MA, USA), a metal union with a conductive perfluoroelastomer ferrule, fittings, a tubing sleeve, a needle port, and a fused silica capillary (IDEX Health and Science, Oak Harbor, WA, USA). High voltage was supplied by a regulated power supply (PS350, Stanford Research Systems, Sunnyvale, CA, USA) (*see* **Note 1**).
2. A syringe pump (Physio 22, Harvard Apparatus, Holliston, MA, USA) and a 500 μL syringe (Hamilton, Reno, NV, USA) were utilized to pump the electrospray solvent through the emitter.

2.4.3 Laser Pulse Delivery

1. A mid-IR optical parametric oscillator, driven by a Q-switched Nd:YAG laser (Vibrant IR, Opotek, Carlsbad, CA, USA), produced 5 ns pulses at 2,940 nm wavelength with a repetition rate of 10 Hz (*see* **Note 2**).
2. The blunt end of fiber was mounted on a miniature 5-axis translator (BFT-5, Siskiyou, Grants Pass, OR, USA) with a bare fiber chuck. The sharpened end was manipulated by a micromanipulator (MN-151, Narishige, Tokyo, Japan).
3. A plano-convex CaF_2 lens with a focal length of 76.2 mm (Infrared Optical Products, Farmingdale, NY, USA) was used to focus the laser beam onto the blunt end of the optical fiber. Care was taken that the laser pulses filled out the entire cross section of the core and did not damage the blunt fiber end.

2.5 Molecular Imaging and Data Analysis

1. An orthogonal acceleration time-of-flight mass spectrometer (Q-TOF Premier, Waters, Milford, MA, USA) was used to acquire mass spectra. The commercial electrospray source was replaced by our fiber-based LAESI source.
2. A three-axis translation stage with motorized actuators and a stage controller (LTA-HS, Newport, Irvine, CA, USA) provided the basis of accurate sample stage movement.
3. The stage movement scanning program, to target the centroids of individual cells based on their coordinates, was written in house using a visual programming platform (LabView, National Instruments, Austin, TX, USA).
4. Software for data analysis and molecular image processing included a scientific visualization package (Origin 8.0, Origin Lab, Northampton, MA, USA), and image processing programs (Photoshop 7.0, Adobe Systems Inc., San Jose, CA, USA, and ImageReady 7.0, Adobe Systems Inc., San Jose, CA, USA).

3 Methods

Automated cell-by-cell imaging by LAESI-MS relies on cell recognition and cell addressing derived from optical microscope images of the sample. For the ablation of individual cells, the centroid coordinates of targeted cells were determined through image processing. A stage-control program was developed to take these coordinates as input and sequentially position individual cells under the fiber tip for ablation. The ablation events for each cell resulted in a mass spectrum that reflected numerous molecular components of the cell. Peak intensities for selected ions were determined to build a false color image of cell-by-cell metabolite distributions in the tissue. Alternatively, cells of different morphologies were selectively targeted for analysis.

3.1 Preparation of Optical Fiber with a Sharpened End

1. 1-Methyl-2-pyrrolidinone was heated to 130–150 °C in a small beaker. A coated germanium oxide (GeO_2)-based glass optical fiber was dipped into the heated solvent for a minute until its plastic coating turned soft and started to peel off. The fiber was removed from the solvent, and quickly dipped into methanol to wash off the coating. Lint-free tissue was used to wipe off any remaining coating.
2. Both ends of the fiber were cleaved using a sapphire scribe (KITCO Fiber Optics, Virginia Beach, VA, USA) by scoring and gently snapping the fiber.
3. For etching, one end of the fiber was held using a bare fiber chuck and positioned vertically using a translation stage. The mounted fiber end was dipped into 1.0–2.4 % (*v/v*) reagent-grade nitric acid to a vertical depth of 0.3–0.5 mm. After ~15 min, when the etching was completed, the fiber tip automatically detached from the acid surface. The etched sharp fiber tip was rinsed with deionized water.

3.2 Cell Coordinate Recognition

1. A microtome knife blade and fine tweezers were used to cut and peel off the abaxial or adaxial epidermal layer of plant tissue. The peeled layer was mounted on a clean microscope slide.
2. A reference marker (i.e., a dot by a waterproof marker pen) was placed on the backside of microscope slide, and the plant (e.g., *L. longiflorum*) epidermis was observed under the upright microscope. A unique cell or feature on the tissue was selected with reference to the marker, and a recognizable point in it was defined as the origin of the coordinate system for the selected tissue area.
3. The defined origin was positioned at the top left corner of the field of view in the microscope. Images of the selected tissue area were captured at different magnifications and with different imaging modes (*see* **Note 3**).
4. Image processing software, e.g., ImageJ or MetaMorph for Olympus, was used to threshold and binarize the microscope image, and accentuate the cell edges. Objects, corresponding to cells, were identified in these binarized images and integrated morphometry analysis was performed to determine the centroids of each object (*see* **Note 4**). The centroid coordinate dataset was exported into the stage-control program for addressing the cells. The cell coordinate recognition process for the cell-by-cell imaging of the adaxial epidermis of *L. longiflorum* leaf is shown in Fig. 1a–c. Figure 2a–c shows the differentiation of two cell types (pavement cells and guard cells) in the abaxial epidermis of an *L. longiflorum* leaf and captures the coordinates corresponding to one of them (guard cells).

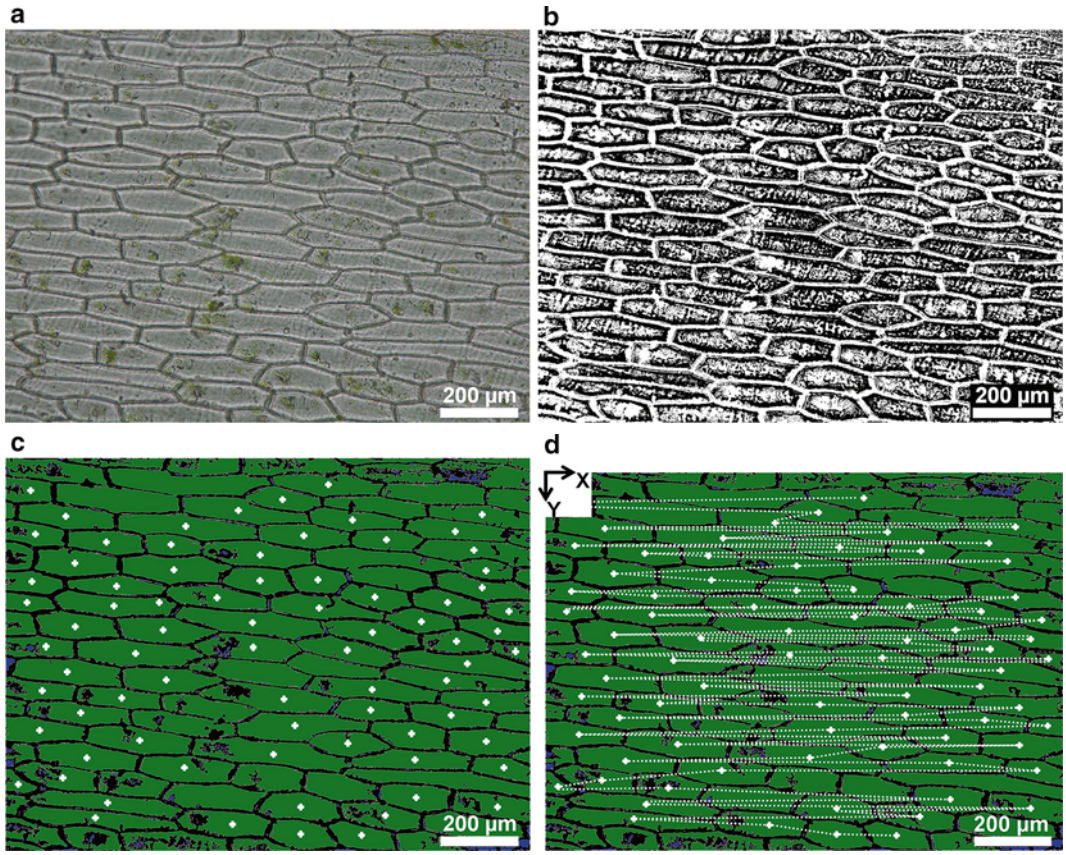

Fig. 1 Coordinate acquisition for single-cell ablation in an optical microscope image of *L. longiflorum* leaf adaxial epidermis. (**a**) Microscope image of *L. longiflorum* leaf adaxial epidermis is taken. (**b**) Cell walls are accentuated by thresholding the grayscale levels. (**c**) The image is binarized and the cells are recognized as objects. Centroids of cells (marked by *plus* signs) are determined. (**d**) Scanning path for the translation-stage movement exposing cell after cell to the ablation fiber is shown by *dashed line*. Origin is at the *top left corner* of the image

3.3 Translation-Stage Automation

1. The three-axis translation stage was configured and initialized through the stage controller.
2. The home position in the *x*–*y* plane and the elevation of the fiber tip in the *z* direction were optimized according to the sample geometry. There were two specific values for the fiber tip elevation. The "operational height" was determined by optimizing the laser ablation efficiency. The "relocation height" was more elevated to ensure unobstructed stage movement from one cell to another during scanning.
3. A set dwell time was determined based on the number of laser pulses needed to ablate a single cell.

3.4 LAESI-MS on Single Cells

1. The microscope slide holding the cell layer (e.g., *L. longiflorum* leaf abaxial epidermis or *A. cepa* epidermis) was carefully moved from the upright microscope to the translation stage in front of the mass spectrometer (*see* **Note 5**).

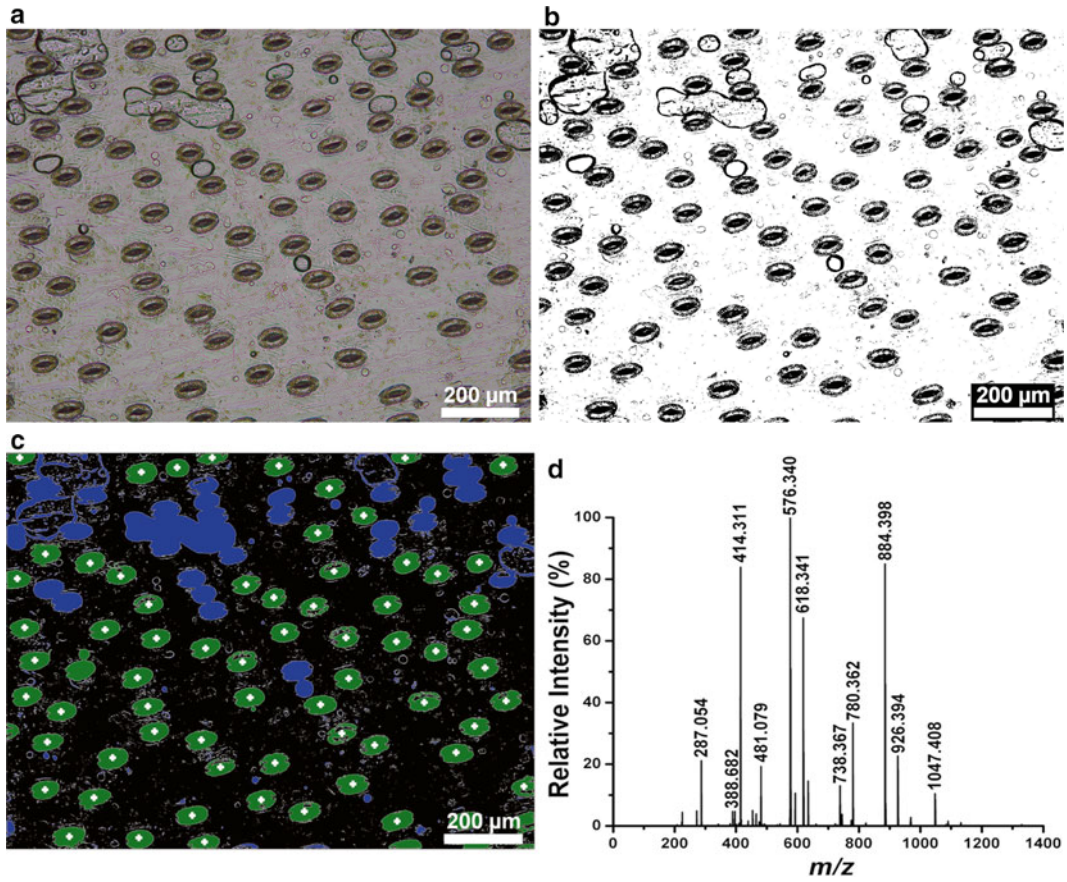

Fig. 2 (**a**) Microscope image of *L. longiflorum* leaf abaxial epidermis. (**b**) Thresholded image showing cell edge detection. (**c**) Centroids of guard cells with distinctive morphology are determined in the binarized image (marked by *plus* signs). (**d**) Mass spectrum of a pair of guard cells

2. The top-view and side-view cameras were adjusted to allow clear observation of the selected tissue and the etched fiber tip.
3. To accurately locate the origin of the coordinate system selected under the imaging microscope and position it under the fiber tip, the unique cell or feature in its environment was found through the top-view camera (*see* **Note 6**).
4. The fiber tip was lowered to a distance of 30–15 µm above the sample surface ("operational height") and adjusted in the *x*–*y* plane to be located above the origin of the coordinate system defined over the sample (*see* **Note 7**).
5. The syringe pump operating at a flow rate of 300 nL/min supplied the electrospray solution to the tapered stainless steel emitter. Stable electrospray was generated by applying a high voltage (2,800–3,000 V) on the metal union of the electrospray system.
6. The cell coordinates and scanning parameters were imported into the stage-control program.

7. The mid-IR laser was initialized and the pulse energy and repetition rate were optimized to enable the highest signal-to-noise ratio in a single-cell mass spectrum without affecting neighboring cells or breaking the fiber tip.
8. Acquisition parameters for the mass spectrometer (e.g., mass range: *m/z* 20–1,500, scan rate: 1 s/scan, positive ion acquisition mode) were selected.
9. The acquisition of mass spectra was initiated.
10. The pulses from mid-IR laser were fired at the first cell and simultaneously the stage-control program was started. The translation stage was directed to present the selected cells one by one to the tip of the ablation fiber. Figure 1d shows the path of movement on the *L. longiflorum* leaf adaxial epidermis.
11. When the data acquisition process was completed, all instrument components, including sample scanning, mid-IR laser, and electrospray, were stopped.

3.5 Cell-by-Cell Images

1. Mass spectra were analyzed to evaluate metabolites levels of individual cells. For example, in an experiment to study the molecular composition of cells with a particular morphology, the mass spectrum from a pair of guard cells of the *L. longiflorum* leaf abaxial epidermis was acquired (*see* Fig. 2d). Ions of interest, such as *m/z* 884.398 and 926.394, were identified as steroidal glycosides by separate tandem MS experiments and were consistent with previous studies [16, 17].
2. For cell-by-cell imaging, the peak intensities of selected ions were traced in ion chromatograms as individual cells were interrogated. The scan numbers in the chromatogram were correlated to the cells in the microscope image.
3. The ion intensities from each ablated cell were measured to construct a false color cell-by-cell molecular image reflecting the metabolite distribution in the tissue. Figure 3c, d shows the cell-by-cell molecular images for selected ions in a monolayer of *A. cepa* epidermis. Mass spectra for nonpigmented and purple cells show significant differences (*see* Fig. 3b for the comparison). The strong correlation of the pigment distribution, e.g., cyanidin malonyl glucoside with *m/z* 535.113 (*see* Fig. 3c), with the coloration of these cells in the optical image (*see* Fig. 3a), validates this cell-by-cell imaging approach. In contrast, a trisaccharide distribution with *m/z* 543.159 does not follow the coloration pattern (*see* Fig. 3d).

4 Notes

1. Direct contact with the high voltage applied to the electrospray emitter can cause electric shock that may result in severe injuries or death. Exposed electrical components were carefully

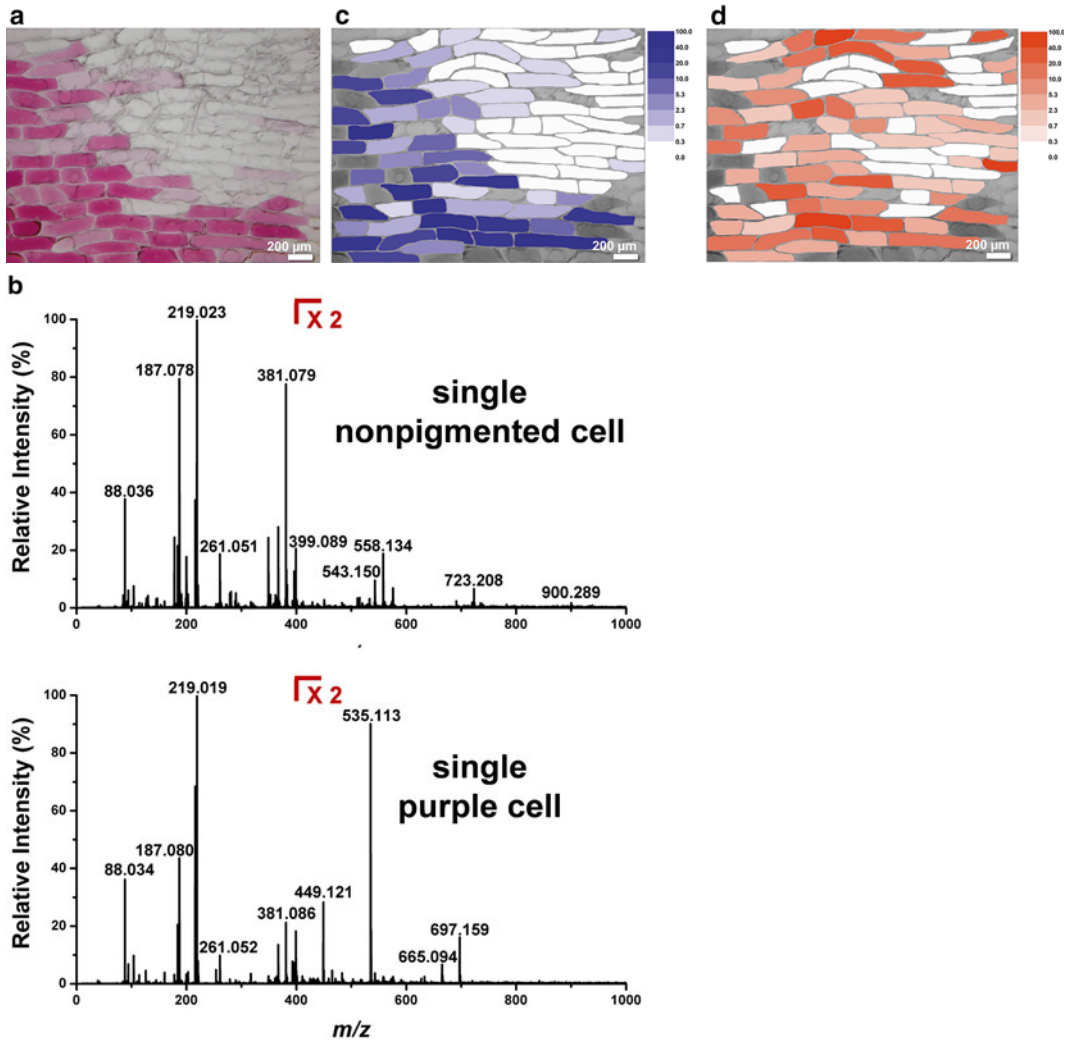

Fig. 3 (**a**) Microscope image of *A. cepa* bulb epidermal tissue showing nonpigmented and purple cells. (**b**) Mass spectra from (*top panel*) a single nonpigmented cell and (*bottom panel*) a single purple cell. (**c**) Cell-by-cell molecular image of cyanidin malonyl glucoside with *m/z* 535.113 is consistent with the distribution of purple color in the optical image (*see* Fig. 3a). (**d**) Cell-by-cell molecular image of trisaccharide with *m/z* 543.159 shows more uniform distribution

shielded and appropriate signs were posted. It was forbidden to approach the high-voltage area during experiments.

2. Appropriate protection from laser beam exposure is necessary, including wearing mid-IR-range laser goggles and clothes with long sleeves.
3. The imaging methods of the upright microscope included bright-field and transmission illumination, and differential interference contrast mode. Images were obtained with high definition of the cell walls to facilitate automatic cell recognition.

4. Integrated morphometry measurements were performed on well-binarized images with clearly differentiated cells as objects. Filter parameters in the image analysis included object area, shape, and orientation to improve the measurement accuracy.
5. The sample slide mounted on the translation stage had to be placed horizontally flat in the *x*–*y* plane to maintain a constant distance between the fiber tip and the tissue surface over the studied area, and prevent the fiber tip from touching the sample during scanning.
6. The origin defined in the imaging microscope had to be found in the top-view observation microscope visualizing the single-cell LAESI experiment. The positioning of images under these two visualization systems had to be consistent and follow the same orientation.
7. Fine control of the distance (~25 μm) between the fiber tip and the sample surface was required for efficient ablation. Touching the sample surface by the etched fiber should be avoided to prevent damage to the cell and/or the fiber tip.

Acknowledgments

The authors acknowledge the financial support from the US National Science Foundation (Grant No. CHE-1152302) and the George Washington University Selective Excellence Fund. The GeO_2-based glass fibers were generously provided by Infrared Fiber Systems (Silver Spring, MD).

References

1. Chaurand P, Schwartz SA, Billheimer D, Xu BJ, Crecelius A, Caprioli RM (2004) Integrating histology and imaging mass spectrometry. Anal Chem 76:1145–1155
2. Miura D, Fujimura Y, Wariishi H (2012) In situ metabolomic mass spectrometry imaging: recent advances and difficulties. J Proteomics 75:5052–5060
3. Watrous JD, Dorrestein PC (2011) Imaging mass spectrometry in microbiology. Nat Rev Microbiol 9:683–694
4. Watrous JD, Alexandrov T, Dorrestein PC (2011) The evolving field of imaging mass spectrometry and its impact on future biological research. J Mass Spectrom 46:209–222
5. Goto-Inoue N, Hayasaka T, Zaima N, Setou M (2011) Imaging mass spectrometry for lipidomics. Biochim Biophys Acta 1811: 961–969
6. Walch A, Rauser S, Deininger S-O, Höfler H (2008) MALDI imaging mass spectrometry for direct tissue analysis: a new frontier for molecular histology. Histochem Cell Biol 130:421–434
7. Wiseman JM, Ifa DR, Song Q, Cooks RG (2006) Tissue imaging at atmospheric pressure using desorption electrospray ionization (DESI) mass spectrometry. Angew Chem Int Ed 45:7188–7192
8. Nemes P, Barton AA, Li Y, Vertes A (2008) Ambient molecular imaging and depth profiling of live tissue by infrared laser ablation electrospray ionization mass spectrometry. Anal Chem 80:4575–4582
9. Nemes P, Barton AA, Vertes A (2009) Three-dimensional imaging of metabolites in tissues under ambient conditions by laser ablation electrospray ionization mass spectrometry. Anal Chem 81:6668–6675

10. Schwamborn K, Caprioli RM (2010) MALDI imaging mass spectrometry: painting molecular pictures. Mol Oncol 4:529–538
11. Nemes P, Woods AS, Vertes A (2010) Simultaneous imaging of small metabolites and lipids in rat brain tissues at atmospheric pressure by laser ablation electrospray ionization mass spectrometry. Anal Chem 82:982–988
12. Altschuler SJ, Wu LF (2010) Cellular heterogeneity: Do differences make a difference? Cell 141:559–563
13. Shrestha B, Vertes A (2009) In situ metabolic profiling of single cells by laser ablation electrospray ionization mass spectrometry. Anal Chem 81:8265–8271
14. Shrestha B, Nemes P, Vertes A (2010) Ablation and analysis of small cell populations and single cells by consecutive laser pulses. Appl Phys A 101:121–126
15. Shrestha B, Patt JM, Vertes A (2011) In situ cell-by-cell imaging and analysis of small cell populations by mass spectrometry. Anal Chem 83:2947–2955
16. Munafo JP, Gianfagna TJ (2011) Quantitative analysis of steroidal glycosides in different organs of Easter lily (Lilium longiflorum Thunb.) by LC-MS/MS. J Agric Food Chem 59:995–1004
17. Munafo JP, Ramanathan A, Jimenez LS, Gianfagna TJ (2010) Isolation and structural determination of steroidal glycosides from the bulbs of Easter lily (Lilium longiflorum Thunb.). J Agric Food Chem 58: 8806–8813

Methods in Molecular Biology 1203

Springer Protocols

Lin He *Editor*

Mass Spectrometry Imaging of Small Molecules

Humana Press

METHODS IN MOLECULAR BIOLOGY

Series Editor
John M. Walker
School of Life Sciences
University of Hertfordshire
Hatfield, Hertfordshire, AL10 9AB, UK

For further volumes:
http://www.springer.com/series/7651

Mass Spectrometry Imaging of Small Molecules

Edited by

Lin He

Department of Chemistry, North Carolina State University, Raleigh, NC, USA

Humana Press

Editor
Lin He
Department of Chemistry
North Carolina State University
Raleigh, NC, USA

ISSN 1064-3745 ISSN 1940-6029 (electronic)
ISBN 978-1-4939-1356-5 ISBN 978-1-4939-1357-2 (eBook)
DOI 10.1007/978-1-4939-1357-2
Springer New York Heidelberg Dordrecht London

Library of Congress Control Number: 2014953846

Printed on acid-free paper

Humana Press is a brand of Springer
Springer is part of Springer Science+Business Media (www.springer.com)